An integrated analysis of the effects of Esculentin 1-21 on Saccharomyces cerevisiae.

Available online at www.sciencedirect.com
ScienceDirect
Biochimica et Biophysica Acta 1774 (2007) 688–700
Biochimica et Biophysica Acta
BBA
www.elsevier.com/locate/bbapap

An integrated analysis of the effects of Esculentin 1–21 on *Saccharomyces cerevisiae*

Tania Gamberi [a,1], Duccio Cavalieri [c,1], Francesca Magherini [a], Maria L. Mangoni [b], Carlotta De Filippo [c], Marina Borro [b], Giovanna Gentile [b], Maurizio Simmaco [b], Alessandra Modesti [a,*]

[a] *Dipartimento di Scienze Biochimiche, Università degli Studi di Firenze, Viale G. Morgagni, 50 I-50134 Firenze, Italy*
[b] *Dipartimento di Scienze Biochimiche, II Facoltà di Medicina, Azienda Ospedaliera Sant'Andrea, Università La Sapienza Roma, Italy*
[c] *Dipartimento di Farmacologia, Università degli Studi di Firenze, Italy*

Received 11 October 2006; received in revised form 3 April 2007; accepted 5 April 2007
Available online 21 April 2007

Abstract

The antimicrobial peptide esculentin 1–21 (Esc 1–21) is a shorter synthetic version of the 46-residue peptide occurring in the *Rana esculenta* skin secretion. Here we propose an integrated proteomic and transcriptomic approach to interpret the biological effects of this peptide on *Saccharomyces cerevisiae*. We further investigated the response to this peptide by correlating the results of the transcriptome and proteome analysis with phenotypic effects. The results show that *S. cerevisiae* adapts to Esc 1–21 using the High Osmolarity Glycerol (HOG) pathway involved in osmotic tolerance and cell wall maintenance. Comparative proteomics reveals that Esc 1–21 causes downregulation of enzymes of the lower glycolytic pathway and in genes involved in spindle body formation and remodelling of cell-wall synthesis. Moreover the peptide induces downexpression of protein actin within 45 min and cells pre-treated with peptide show less sensitivity to osmotic stress and increased sensitivity to heat shock stress. The results obtained with the two different methodologies are in agreement at the cellular process levels. A combined approach may help elucidate the main aspects related to the effects of this peptide on the eukaryotic cell. The employment of different technologies may reveal the potential and limitations of each adapted approach in a prospective application for drug screening.

Keywords: *S. cerevisiae*; Systems biology; Proteomic; Transcriptomic; Antimicrobial peptide

1. Introduction

Some multicellular organisms in the phylogenetic tree produce a variety of different compounds as an early protective response against bacteria, fungi and viruses, which constitutes the so-called innate immune system. In addition, higher eukaryotes have evolved a sophisticated defense system comprising a complex network of humoral and cellular responses, called "adaptive immunity" [1]. Innate immunity was discovered in the early 1980s and gene-encoded antimicrobial peptides (AMPs) represent its major component in all living organisms, where they act as a first barrier against a broad range of invading pathogens [2,3]. Accordingly, they are located at the anatomical sites primarily involved in contact with microorganisms, such as mucosal, epithelial or phagocytic cells [4–6]. Although AMPs differ significantly in their sequences, most of them share some features, such as a high positive charge and a potential to adopt an amphipathic α-helix and/or β-sheet structures upon interaction with membranes [7]. To date, there is compelling evidence that a common step in the microbial killing mechanism is the electrostatic interaction of AMPs with the negatively charged cell membrane followed by its permeation/disruption [8] or with the actin cables of the cytoskeleton [9]. The amphibian skin secretions constitutes one of the richest sources of AMPs that are synthesized and stored within granules of holocrine-type serous glands and released upon stimulation [10,11]. Among the skin secretions of *Rana esculenta*, the esculentin-1 family of peptides, (containing 46-amino acids with a C-terminal hepta-

* Corresponding author. Fax: +39 055 459 8905.
E-mail address: modesti@scibio.unifi.it (A. Modesti).
[1] These two authors contributed equally to this work.

1570-9639/$ - see front matter © 2007 Elsevier B.V. All rights reserved.
doi:10.1016/j.bbapap.2007.04.006

membered ring stabilized by a disulphide bridge), is the most potent, being active against both Gram-positive and Gram-negative bacteria, yeasts and filamentous fungi, with negligible effects on eukaryotic cell membranes [12]. It has already been reported that the antimicrobial activity of the esculentin-1a is located in its N-terminal portion and that at least the first 18 residues are required for its antimicrobial properties [13]. Therefore, to better investigate the antifungal activity of esculentin, we synthesized a shorter analogue containing 21 amino acids and tested it against *Saccharomyces cerevisiae.* This peptide was named esculentin-1a (1–21) (Esc 1–21), since it shares the first 20 residues with the natural esculentin-1a. Differently from Esc 1–18, Esc 1–21 carries the substitution Leu 11 Ile and three additional C-terminal residues (Leu–Lys–Gly) which give it a higher net positive charge and a length which is optimal, for an alpha-helical peptide, to span the phospholipid bilayer (Table 1). During the last few years, a considerable number of studies have been carried out with AMPs on bacteria, fungi, viruses and tumor cells, in an attempt to understand the parameters responsible for their mechanism of action. Nevertheless, reports on the gene and protein expression profile of cells exposed to a sub-lethal peptide concentration are still very scarce. In this study we used *S. cerevisiae* as a model to study the mechanisms of action of Esc 1–21 using an integrated approach. The choice of yeast as a model is based on several considerations: it is one of the key model genetic organisms and a great deal is known about its molecular biology, cell biology, metabolism and physiology. More generally, it has been demonstrated that about 900 genes are part of common environmental stress response (ESR) to several unrelated environmental challenges [14]. *S. cerevisiae* has also been extensively used for whole genome approaches investigating the effect of drugs on the transcriptome [15]. Yeast has also been the model of choice for proteomic studies using 2D gels and mass spectrometry to characterize the response to different stressors [16] or to the expression of specific genes [17]. Nevertheless studies investigating the effects of drugs on the proteome and/or both on the proteome and the transcriptome have not been conduced in an integrated manner.

Here we describe the effect of Esc 1–21 on yeast cell biology by measuring cell viability and growth rate. At the same time we elucidate the genomic determinants of these effects, through analysis of the proteome and transcriptome. The results obtained show that Esc 1–21 slows down yeast growth without causing cell death by affecting the expression of specific genes and therefore, by modulating the synthesis of many proteins involved in rerouting the metabolism of cell membranes and cell bioenergetics. Our results demonstrate that 2-DE electrophoresis combined with mass spectrometry and gene expression provide a useful approach to profiling antimicrobial peptides according to their protein and gene expression patterns.

2. Materials and methods

2.1. Peptide and yeast strain and media

Synthetic Esc1–21 were purchased from SYNT:EM (Nimes, France). The peptide solution was prepared in 20% ethanol at a final concentration of 1.2 mM. The yeast strain used in this study was *S. cerevisiae* W303-1A (*MATa, leu2-3,112ura3-1 trp1-92 his3-11, 15 ade2-1 can1-100, GAL SUC mal*). The growth medium used was YEPD (*y*east *e*xtract, 1%; *p*eptone, 2%; *d*extrose, 2%). All media and reagents were from Merck.

2.2. Measurement of growth inhibition activity

The antifungal activity of the peptide was assayed by microspectrophotometry of liquid culture growth in 96-well microtiter plates for 24 h by measuring optical density at 640 nm with a Victor high throughput microplate spectrophotometer equipped with a 96-well plate reader (Perkin Elmer) [18]. Briefly exponential-phase cells were harvested and suspended in 0.2 ml of liquid YEPD (0.1×10^7 cells/ml) containing 10, 25, 50 μM of Esc 1–21 or 0% v/v, 0.4% v/v, 0.8% v/v of ethanol as control.

To assess the viability of yeast cells, exponentially growing W303-1A cells were diluted to 0.8×10^7 cells/ml in liquid YEPD medium containing 25, 50 and 100 μM of Esc 1–21. After incubation for 0, 3, 6 and 9 h at 30 °C, the cells were plated on YEPD without peptide for 2 days at 30 °C.

2.3. Effect of hyperosmotic or heat stresses on peptide sensitivity

To analyze the effect of hyperosmotic stress on Esc 1–21 sensitivity 0.8×10^7 cells/ml were pre-treated in liquid YEPD with different concentrations of peptide (25, 50, 100 μM) for 0 and 3h and plated after appropriate dilutions on YEPD agar and YEPD agar supplemented with 0.6 M sorbitol and without peptide for 2 days at 30 °C. Osmotic tolerance was expressed as the percentage of cells able to grow on YEPD agar supplemented with 0.6 M sorbitol compared to those growing on YEPD agar.

To analyze the effect of heat stress on Esc 1–21 sensitivity, 0.8×10^7 cells/ml were treated with different concentrations of peptide (25, 50, 100 μM) for 0 and 3 h and after incubation were divided into two aliquots. An aliquot was plated on YEPD agar as a control; another aliquot was heated for 20 min at 52 °C. After cooling, cells were spread on YEPD agar without peptide. Colonies were counted after 2 days at 30 °C. Heat stress resistance is expressed as the percentage of cells able to give rise to colonies after heating compared to the control.

2.4. Preparation of yeast cell extracts for 2D electrophoresis

W303-1A yeast cells (0.8×10^7 cells/ml) were treated with 50 μM Esc1–21 in liquid YEPD and incubated at 30 °C with shaking for 45 (T1) and 90 (T2) min. Treated and untreated cells were harvested by centrifugation at room temperature. The pellet was washed twice in water and resuspended in 8 M urea, 4% (w/v) CHAPS and 10 mM DTT. Cells were broken with glass beads in a Fastprep instrument (Savant) and lysates were clarified by centrifugation at

Table 1
Amino acid sequences and net charge of esculentin

Peptide	Sequence [a]	Net charge
Esculentin-1a	GIFSKLAGKK**I**KNLLISGLKNVGKEVG**M**DVVRTGIDIAGCKIKGEC	+6
Esculentin-1b(1–18)	GIFSKLAGKK**L**KNLLISG-NH_2	+5
Esculentin-1a(1–21)	GIFSKLAGKK**I**KNLLISGLKG-NH_2	+6

Amino acid sequences and net charge of esculentin-1a (natural peptide), esculentin-1b(1–18) and esculentin-1a(1–21) corresponding to the first 21 residues of esculentin-1a.

[a] Amino acid substitutions are boldfaced.

13,000 rpm for 10 min. The protein concentration was determined by BCA assay (Pierce Biotechnology, Inc).

Two-dimensional electrophoresis—2-DE was performed using the Immobiline polyacrylamide system as described in [17]. Briefly, 60 μg (analytical) or 500 μg (preparative) of protein sample were applied on a commercial non-linear immobilized pH gradient from pH 3 to pH 10, of 18 cm length (Amersham Biosciences, Uppsala, Sweden). Isoelectric focusing was carried out on the Ettan™ IPG phor™ system (Amersham Biosciences). IPG strips were rehydrated in 350 μL of lysis buffer and 0.2% (v/v) carrier ampholyte for 1 h at 0 V and for 8 h at 30 V, at 16 °C. The strips were focused according to the following electrical conditions at 16 °C : 200 V for 1 h, from 300 to 3500 V in 30 min, 3500 V for 3 h, from 3500 to 8000 V in 30 min, and 8000 until a total of 80,000 V/h was reached. Following IEF separation, the strips were equilibrated with 10 ml of a solution containing 50 mM Tris–HCl pH 6.8, 6 M urea, 30% (v/v) glycerol, 2% (w/v) SDS and 2% (w/v) DTE for 12 min and with 10 ml of a solution containing 50 mM Tris–HCl pH 6.8, 6 M urea, 30% (v/v) glycerol, 2% (w/v) SDS, 2.5% (w/v) iodoacetamide and a trace of bromophenol blue for 5 min. The IPG strips were then placed on 12% SDS –PAGE gels (18 cm × 20 cm × 1.5 mM) and overlaid with a solution of 0.5% (w/v) agarose. The second-dimensional SDS-PAGE was carried out at 40 mA *per* gel constant current, at 10 °C, until the dye front reached the bottom of the gel. Analytical gels were stained with ammoniacal silver nitrate as previously described [19]. The MS-preparative gels were stained according to a silver staining protocol compatible with MS [20]. Volume ratio of the spot observed in the different 2-DE patterns was obtained using the differential analysis tool of Melanie 4 software (GeneBio, Geneva, Switzerland). For the proteomics experiments we performed three independent biological repetitions and three technical replicates of the 2-DE gels for each experimental condition.

2.5. Protein identification by peptide mass fingerprinting (MALDI-ToF MS)

Protein spots of interest were manually cut out of the gel and destained in 30 mM potassium ferricyanide/100 mM sodium thiosulfate/H_2O solution (1:1:2, by vol.). Gel pieces were then washed 6 times with deionized water, equilibrated with 200 mM ammonium bicarbonate for 20 min, washed with deionized water, dehydrated twice with acetonitrile for 20 min and in-gel digested with trypsin (Trypsin Gold, mass spectrometry grade, Promega) according to the manufacturer's protocol. Peptides were extracted from the gel with 50% acetonitrile/ 5% trifluoroacetic acid (2 steps, 20 min at RT each), dried, resuspended in 0.1% trifluoroacetic acid and purified with micro ZipTip C18 pipette tips (Milllipore, Billerica, MA) eluting directly in the matrix solution (10 mg/ml cyano-4-hydroxycinnamic acid in 50% acetonitrile/1% TFA). The mass spectra of the tryptic peptides were obtained using a Voyager-DE MALDI-ToF mass spectrometer (Applied Biosystems). Peptide mass fingerprint database searching was carried out using the PeptIdent algorithm (http://www.expasy.org) in the SWISS-PROT and TrEMBL databases, setting the parameters to allow one missed cleavage and a mass tolerance of 1 Da.

2.6. Analysis of the actin cytoskeleton

Cells (0.8×10^7 cells/ml) were treated with 50 μM Esc 1–21 in liquid YEPD and incubated at 30 °C with shaking for 45 min. Treated and untreated cells were harvested by centrifugation at room temperature. The pellet was washed twice in water and resuspended in RIPA buffer (50 mM Tris–HCl pH 7.5, 150 mM NaCl, 5 mM EDTA, 1% NP-40, 1 mM PMSF, and 2 μg/ml each of aprotinin, pepstatin A and leupeptin (Sigma-Aldrich)). Cells were broken with glass beads in a Fastprep instrument (Savant) and lysates were clarified by centrifugation at 13,000 rpm for 10 min. The protein concentration was determined by BCA assay (Pierce) and 40 μg of total proteins (per gel lane) from each lysate were mixed with Laemmli buffer and incubated al 95 °C for 5 min before running on a 12% polyacrylamide gel. After standard SDS-PAGE, proteins were transferred to a polyvinylidene-difluoride membrane (PVDF by Immobilon P; Millipore, Bedford, MA) and incubated with anti-actin goat polyclonal antibody (Santa Cruz Biotechnology, CA) diluted 1:1000 in blocking solution and incubated overnight at 4 °C. After three washes in phosphate-buffered saline solution with 0.5% Tween-20, the blots were developed using a chemiluminescence detection system (ECL method by Amersham Biosciences).

2.7. Microarray hybridization

The yeast oligonucleotide array was constructed using the *S. cerevisiae* Genome Oligo Set ™ (Operon Technologies, CA, USA) composed of 6240 optimized oligonucleotides (70mers) each representing one yeast gene. The lyophilized oligonucleotides were resuspended in 3× SSC solution and printed using the microarrayer Omnigrid 100 (Genomic Solutions, Ann Arbor, MI, USA) on poly-L-lysine glass slides (Erie Scientific Company, Portsmouth, NH, USA). After printing, microarrays were post-processed following DeRisi's laboratory procedure (http://derisilab.ucsf.edu/).

Yeast cells were treated with Esc 1–21 as described. RNA was extracted from about 3×10^8 cells using hot acid phenol-chloroform. Nucleic acids were ethanol precipitated, washed, dried, and resuspended in TE buffer. Yield ranged from 2 to 3 mg, with a 260 nm/280 nm absorption ratio of 1.8–2.2. mRNAs were purified using Extraction Kit from Qiagen (Valencia, CA). The microarray hybridization protocols were optimized from those reported in [28], using the indirect labeling method. Briefly, the reactive amine derivative of dUTP, 5-(3-aminoallyl)-2′-deoxyuridine 5′-triphosphate (Sigma) was incorporated into cDNA using the Superscript II reverse transcriptase (Invitrogen) and oligo dT (Invitrogen) and random examers (Roche). After synthesis of cDNA (2–3 h at 42 °C), RNA was hydrolyzed by addition of sodium hydroxide and EDTA to a final concentration of 100 mM and 10 mM, respectively and incubated at 65 °C for 10 min. The hydrolysis reaction was neutralized with 1 M HEPES. After removing free nucleotides by purification and concentration using Microcon-30 microconcentrators, the aminoallyl-labeled samples were coupled to succinimidyl ester of cyanine-3 (Cy3) and cyanine-5 (Cy5) (Amersham) combined with 1 M $NaHCO_3$, pH 9. Coupling took place in the dark at 25 °C for 1 h. Appropriate Cy3 and Cy5 labeled cDNA samples were purified following Qiagen Qiaquick PCR Purification Kit instructions. Poly-dA (12–18 mer), 20× SSC, and HEPES pH 7.0 were added. After the resultant mix was filtered through a Millipore 0.45 μM filter, 10% SDS was added. The samples were incubated for 2 min at 100 °C and cooled in a microcentrifuge prior to loading and then applied to microarray. Incubation took place at 65 °C for 12–15 h. Hybridized slides were washed in a solution of water, 20× SSC, and 10% SDS, rinsed in water and 20× SSC, and dried via centrifugation for 2 min at 1000 rpm. The arrays were scanned immediately. Each comparison was performed in duplicate.

2.8. Gene expression analysis

Fluorescent cDNA bound to the microarray was detected with a GenePix 4000 microarray scanner (Axon Instruments, Foster City, CA), using the GenePix 4000 software package to quantify microarray fluorescence. Intensity values were adjusted by subtracting surrounding background from spots. The median of spot intensities was corrected for background. To eliminate signals that are most prone to estimation error, any spot was excluded from analysis if both the Cy3 and Cy5 mean fluorescence signals were within two standard deviations of the mean background signals for that spot. This procedure avoids artificially inflated measurements of expression due to low signals. Additional to eliminating flagged spots, spots were also visually inspected and flawed ones discarded from the analysis. Data were normalized to mean ratio intensity. Genes within each group were examined for functional enrichment using Gene Ontologies categories (GO) and KEGG metabolic pathways using hypergeometric statistics as implemented in Pathway Processor [21,22]. Functional annotations of the metabolic pathways were obtained from KEGGhttp://www.genome.ad.jp/kegg). Mips categories were used to improve yeast classification data. Yeast deletion data were obtained from (http://mips.gsf.de/projects/fungi/yeast.html).

3. Results

3.1. Esculentin 1–21 has antifungal activity

To analyze the molecular basis of the effect of Esc 1–21, we focused on W303-1A, a *S. cerevisiae* strain well characterized both at the proteomic and the gene expression level.

W303-1A cells in exponential phase were treated with increasing concentrations of peptide (10, 25 and 50 μM). As shown in Fig. 1 (panel A), 50 μM Esc 1–21 inhibited cell growth, while 25 μM concentration just slightly decreased the strain growth rate in liquid medium. As evident from the figure, the incubation with 25 μM of peptide caused a decrease of only 23% of the growth rate up to 3 h of treatment in comparison to the control. The cells treated with 50 μM of Esc 1–21 showed a significant and more prolonged reduction in growth rate of about 77% up to 6 h of incubation.

The effect of Esc 1–21 on cell viability, measured as the ability of the cells to give rise to colonies, was tested after the growth in liquid medium containing various concentrations of antimicrobial peptide, for different times, as described in Materials and methods. All cells were still able to form colonies after 3 h of treatment with 25 μM Esc 1–21 (Fig. 1 panel B). The results indicate that this peptide concentration induced cell growth arrest instead of cell death. A more significant effect on growth is obtained when 50 μM Esc 1–21 was used, resulting in almost 30% of cells unable to form colonies after 3 h of incubation. To investigate whether a higher concentration of Esc 1–21 induced cell death, the viability of yeast cell following treatment with 100 μM Esc 1–21 was evaluated. As shown in Fig. 1 (panel B) the growth arrest observed was fairly rapid: less than 50% of the cells were still able to form colonies after 3 h, indicating that in this condition concentration required for 50% growth inhibition (IC_{50}) was 100 μM. In any conditions, after 6 h, the effect on growth inhibition disappeared and the surviving cells restarted to grow. The cells treated with Esc 1–21 at different times showed alterated morphology. The cell abnormalities were mainly wrinkling of the surface.

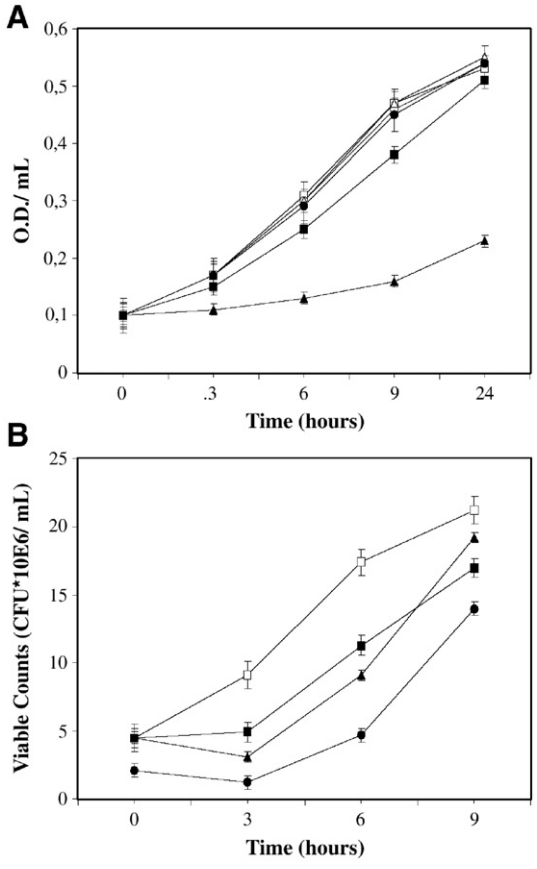

Fig.1. Growth inhibition by Esculentin 1–21. (A) Sensitivity of W303-1A yeast cells to Esc1–21. Exponentially growing cells were diluted to 0.1×10^7 cells/ml in liquid YEPD and treated with different Esc1–21 concentrations for 24 h at 30 °C. Growth rate of treated (● 10 μM, ■ 25 μM, ▲ 50 μM) or untreated (□ 0% v/v, ○ 0.4% v/v, △ 0.8% v/v of ethanol) cells was determined by OD measurements at 600 nm for the indicated times. (B) Cell viability. W303-1A cells were incubated in liquid YEPD cultures with different Esc1–21 concentrations (■ 25 μM, ▲ 50 μM, ● 100 μM) or ethanol 0.8% v/v as control (□) for 9 h at 30 °C. Aliquots were removed at time intervals, diluted and plated on YEPD without peptide for viable cell counts. Values represent the mean of three determinations ± SD.

These features appeared immediately when the cells were treated with 100 μM of peptide but, as observed in viability data, after 6 h the surviving cells exhibited morphology similar to the control (data not shown). We can conclude that 25 μM Esc 1–21 induced reversible cell growth arrest instead of cell death, while higher concentrations such as 100 μM, resulted in 50% of cell death. No TUNEL staining was observed in all the cells, indicating that the phenotypes observed are not associated with cell death by apoptosis (data not shown).

3.2. Esculentin 1–21 treatment induces an increase in osmotic tolerance and a decrease in heat stress resistance

It is well known that osmotic support suppresses the toxicity of a killer toxin [23] and that osmotic stabilizers suppress cell wall lysis [24]. Recent studies indicate that an antifungal agent (Calcofluor) induces an intracellular response related to osmoregulation causing an increase in intracellular glycerol concentration and osmotic tolerance. This effect is a consequence of cell wall perturbation [25]. To test whether the growth arrest and morphology alteration by Esc 1–21 are the consequence of cell wall damage or defects we evaluated the osmotic tolerance by pre-incubating early logarithmically growing cells (0.8×10^7 cells/ml) in liquid YEPD supplemented with different concentrations of Esc 1–21 and determined their osmotic tolerance (as described in Materials and methods) at different times. Osmotic tolerance is expressed as the percentage of cells able to grow on YEPD plates without peptide and supplemented with 0.6 M sorbitol compared to those growing on YEPD alone. Esc 1–21 pre-treatment induced osmotic tolerance in a time- and concentration-dependent fashion in the W303-1A strain, as shown in Fig. 2 (panel A). The yeast cells pre-treated with 100 μM Esc 1–21, which induced 50% of cell death, showed high osmotic tolerance; in fact, after 3 h at this concentration, the basal levels of osmotic tolerance were about 3fold increased in comparison to the control cells at the same time (3 h). As evident from the figure, at 25 or 50 μM of Esc 1–21 concentrations at 3 h of treatment, the increment in the osmotic tolerance was not seen. These results indicate that Esc 1–21 pre-treatment triggers hyper-osmotic shock response although only at the highest concentration tested.

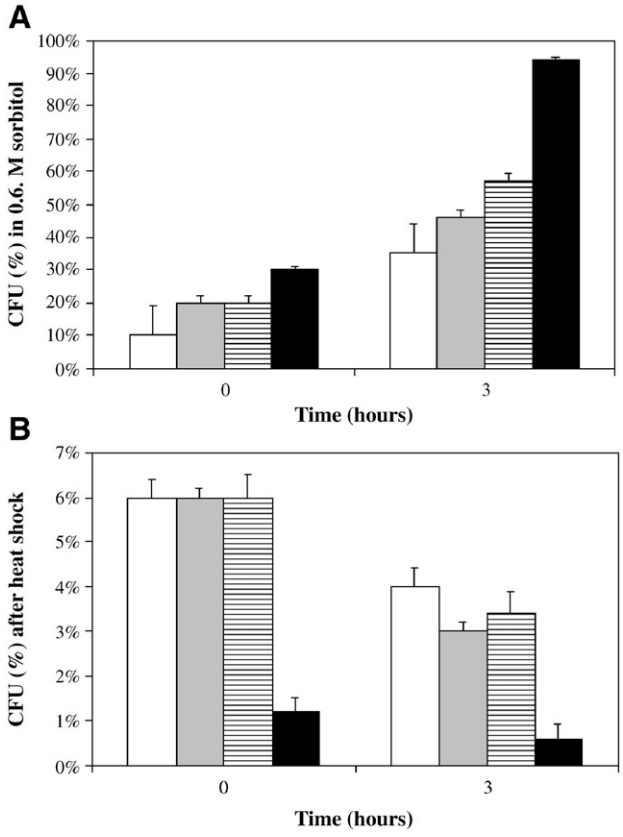

Fig. 2. Osmotic tolerance and heat stress resistance after Esc 1–21 treatment. (A) Osmotic tolerance of W303-1A logarithmically growing culture in liquid YEPD with ethanol 0.8% v/v as control (white) or with Esc1–21 25 μM (gray), 50 μM (hatched) and 100 μM (black) at 0 time and after 3 h of treatment. Osmotic tolerance is expressed as the percentage of cells able to grow on YEPD agar supplemented with 0.6 M sorbitol compared to those growing on YEPD agar and both without peptide. Values represent the mean of three determinations± SD. (B) Heat stress resistance of W303-1A logarithmically growing culture in liquid YEPD and in presence of ethanol 0.8% as control (white) or with Esc1–21 25 μM (gray), 50 μM (hatched) and 100 μM (black) at 0 time and after 3 h of treatment. Heat stress resistance is expressed as described in Materials and methods and spreading the pre-treated cells on YEPD agar without peptide. Values represent the mean of three determinations ±SD.

Like osmotic stress, temperature stress is also known to inhibit cell growth in budding yeast [26]. In order to investigate the effect of Esc 1–21, we evaluated the heat shock resistance of the logarithmically growing cells (0.8×10^7 cells/ml) in liquid YEPD at 30 °C supplemented with different concentrations of Esc 1–21. As shown in Fig. 2 (panel B), W303-1A cells treated with 100 μM Esc 1–21 displayed a dramatic decrease in heat stress resistance in comparison to the control. The yeast cells pretreated with 25 or 50 μM of peptide showed 75% and 80% respectively, of cell viability after heat shock.

From the data presented in Fig. 2 (panel A and B), it can be concluded that pre-treatment of W303-1A cells with 100 μM Esc 1–21 clearly resulted in an increase of osmotolerance and a decrease in heat stress resistance, leading us to conclude that, for this yeast strain, osmotic tolerance and heat stress response are anti-correlated. These results suggest that Esc 1–21 could act on yeast cell wall integrity by inducing a response similar to that elicited from osmotic shock [27].

3.3. Comparison of the 2D gel patterns of the treated and untreated yeast cells and identification of protein variations

Although the molecular details of the yeast growth arrest under peptide exposure are still unknown and in order to understand the proteins involved in the response to Esc 1–21, we investigated the changes in the proteomic pattern. To characterize this Esc 1–21 response, exponentially growing cells were treated with 50 μM peptide for 45 and 90 min. These

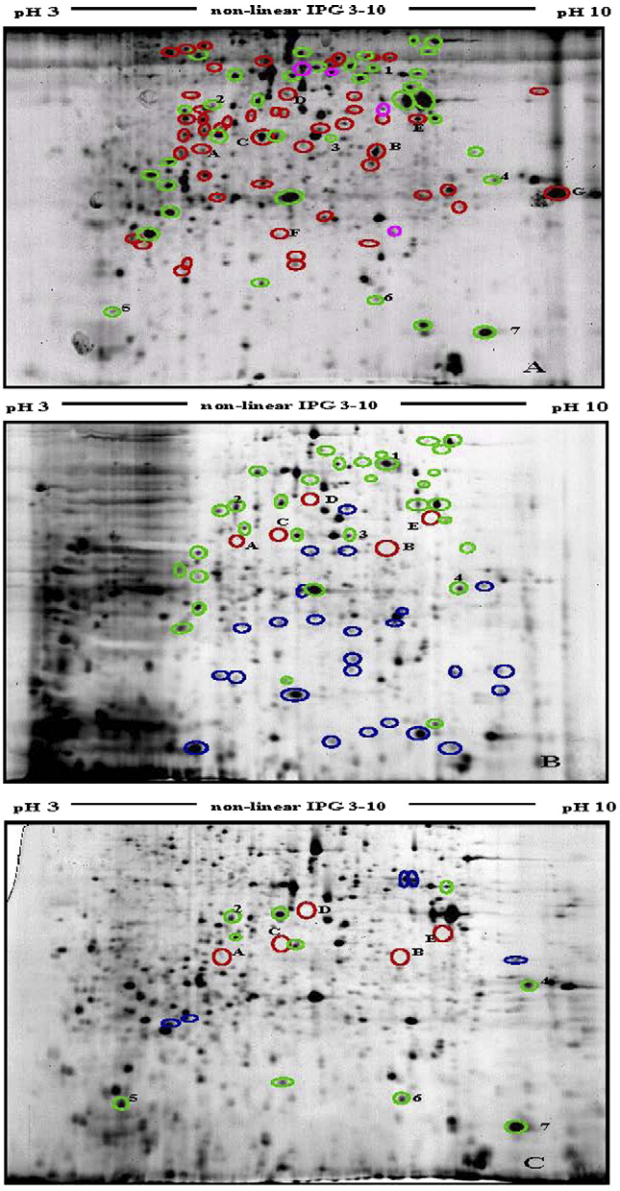

Fig. 3. 2D profiles of protein abundance during Esc 1–21 treatment. A representative 2DE gel of the yeast cells treated with 50 μM of Esc 1–21 for 45' (panel B) or 90' (panel C) and untreated (panel A). Green circles represent proteins increasing or decreasing more than 3fold (quantitative differences) in figure treated cells. Green circles with numbers represents spots up-regulated in T1 and T2. Red, Blue and Magenta circles indicate qualitative differences corresponding to spots present in the control cells in comparison to T1 (Red circles) or in comparison to T2 (Magenta circles). Blue circles represent spots present only in the treated cells (T1 and T2) in comparison to the control. Red circles with capital letters indicates the MS identified proteins indicate the qualitative differences corresponding to spots disappearing both in T1 and T2.

conditions were chosen because previously we found (see above) that 0.8×10^7 cells treated with 50 μM of peptide for 3 h, showed a reversible growth inhibition phenotype with about 70% viable cells. Extracts from control and treated cells were than subjected to comparative two-dimensional gel electrophoresis. The analysis were performed in triplicate to determine whether the relative protein expression changes for Esc 1–21 treatment at 45 (T1) (Fig. 3, panel B) or 90 (T2) min (Fig. 3, panel C) versus control (Fig. 3, panel A) were statistically relevant. Significant differences were found between 45 and 90 min of treatment as shown in Fig. 3. The corresponding 2-DE gels from control at 45 (T1) and 90 (T2) min did not show differences in the protein expression (data not shown). A total of 134 spots, (108 in T1 and 26 in T2) were changed, and 14 of these spots were found in common between T1 and T2 of the treated cells, of which 4 in T1 and 5 in T2 were up-regulated (panels B and C green circles and numbers); 29 (T1) and 5 (T2) spots were down-regulated (panels B and C green circles); 25 and 5 (T1 and T2 respectively) spots were present only in the treated cells (panels B and C blue circles). Fifty in T1 (panel A red circles) and 11 in T2 (panel A magenta circles and red circles with capital letters) were totally unexpressed in comparison with the control. Six spots found in common between gels from T1 and T2 represented proteins which expression was not detectable on 2D gels from Esc 1–21 treated cells both in T1 and in T2 in comparison to the control. These spots (panel A red circles and capital letters and Table 2) were identified. For this study, only unique and deleted expression protein spots in both T1 and T2 gels, in comparison to the control, were chosen for MS analysis. Most of these identified proteins were enzymes involved in the lower part of glycolysis like enolase (spot C), alcohol dehydrogenase I (spot B), pyruvate kinase (spot E) and pyruvate decarboxylase (spot D) , suggesting a lower fermentative capacity in the Esc 1–21-treated cells, probably due to a drop-out of total protein expression. We also identified actin, another protein repressed by Esc 1–21 (Fig. 3 panel A and Table 2 spot A). It is known that there is a correlation between growth arrest, morphological changes and perturbations of actin cytoskeleton. The decrease in actin level suggests that Esc 1–21 affects the integrity of the plasma membrane, resulting in dramatic changes in cell physiology. To further verify the effect of drug treatment on actin expression levels we analyzed treated and untreated cell extracts by Western blot using anti-actin goat polyclonal antibody. The results are shown in Fig. 4 in which it is evident that the expression of actin is dramatically repressed after 45 min of treatment with Esc 1–21 (lane D) in comparison with time 0 (lane B) or the corresponding controls (lane A, time 0 and lane C, 45 min).

3.4. Expression profiling of yeast cells treated with Esc 1–21

Whole expression analysis with DNA microarrays was used to further characterize the response to Esc1–21. Expression analysis was performed on an aliquot of cells processed in parallel to that used to generate 2D gel patterns. After 45 (T1) and 90 min (T2) of treatment with 50 μM Esc 1–21 cells were harvested and the whole genome expression changes were analyzed through comparative hybridization to oligonucleotide arrays of mRNA extracted from treated versus untreated cells [28]. A total of 5240 genes were significantly expressed in the two experiments (data not shown). Since we were analyzing our results at the cellular network and pathway level, we

Table 2
Proteomic and transcriptomic results of qualitative differences in treated cells

Spot	Gene name	Proteomic result	AC[a]	Theoretical Mr/pI[b]	Score[c]	T1[d]	T2[e]	Description
A	ACT1	Absent	P60010	41689.63/5.44	77	1.17	1.01	Actin
B	ADH1	Absent	P00330	36691.94/6.26	52	−1.47	−1.06	Alcohol dehydrogenase
	ADH2					−1.54	−1.21	Alcohol dehydrogenase II
	ADH3					−1.36	1.17	Alcohol dehydrogenase isoenzyme III
	ADH4					1.13	1.36	Alcohol dehydrogenase isoenzyme IV
	ADH5					−2.05	1.12	Alcohol dehydrogenase isoenzyme V
	ARP2					1.14	−1.05	Actin-related protein
	ARP3					−1.36	1.04	Actin-related gene
	ARP4					1.05	1.23	54.8 kDa actin-related protein
	ENO1					−1.36	1.10	Enolase I
C	ENO2	Absent	P00925	46782.98/5.67	66	−1.83	1.28	Enolase
	HPR5					1.19	1.20	DNA helicase
D	PDC1	Absent	P06169	61364.20/5.80	65	−1.39	1.03	Pyruvate decarboxylase
	PDC2					−1.14	−1.34	Asparagine and serine-rich protein
	PDC5					−1.09	−1.05	Pyruvate decarboxylase
E	PYK1	Absent	P00549	54544.63/7.56	74	1.04	1.23	Pyruvate kinase
	PYK2					−1.14	1.11	Pyruvate kinase, glucose-repressed isoform
	SFA1					−1.19	−1.07	Glutathione-dependent formaldehyde dehydrogenase

In the table are listed the MS identified proteins reported in Fig. 3 and the corresponding genes.
[a] SwissProt/TrEMBL accession number.
[b] Predicted pI and Mr according to protein sequence.
[c] Score is $-\log_{10}(P)$, where P is the probability that the observed match is a random event; protein scores greater than 50 are significant ($p<0.05$). It is based on SwissProt database using MASCOT searching program (Matrix Science, London, UK; http://www.matrixscience.com).
[d,e] T1 and T2 are the ratio values of expression measured using DNA microarrays, after 45 (T1) and 90 min (T2) of treatment with 50 mM Esc 1-21, realtive to the untreated control.

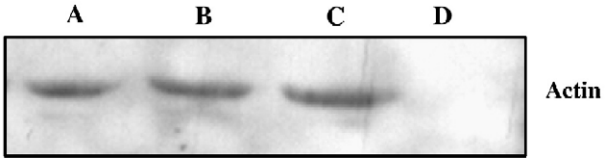

Fig. 4. Analysis of the actin cytoskeleton. Western blot analysis of an extract of: W303-1A control strain treated with ethanol 0.8% v/v for 0 or 45 min (lanes A and C) and W303-1A treated with Esc1- 21 50 μM for 0 or 45 min (lanes B and D). Expression of actin was detected using anti-actin goat polyclonal antibody as described in Materials and methods.

focused on the 940 genes altered more than ±1.5fold to capture a number of connected significant effects (Supplementary Table 1).

Only 100 genes are in common between T1 and T2 (Supplementary Table 2). The decrease in number of genes altered in T2 is in agreement with the proteomic analysis results and the recovery also observed in terms of growth rate.

We further analyzed the expression profiles of cells in T1 and T2, scoring significant enrichment for functional categories, as annotated in KEGG, MIPS, GO and BioCYC (see Materials and methods for details). The significance of calling the entire class of genes up-regulated was assessed using the Fisher's Exact Test, calculated with the hypergeometric distribution, whereby the genes belonging to each annotated class were extracted and visualized using an updated version of the Pathway Processor software (http://:www.ducciocavalieri.org/pathway%20processor) (Table 3). The pathway-based

Table 3
Pathway processor results

[a]Genes in Pathway present in the Data File	[b]T1 Genes exceeding Fold Change Cutoff (−1.8, 1.8)	[c]T1 Signed F.E.T	[b]T2 Genes exceeding Fold Change Cutoff (−1.8, 1.8)	[c]T2 Signed F.E.T	Pathway
39	10	0.0000	5	−0.0017	Carbohydrate- lipid biosynthesis defects
22	6	0.0003	3	0.0129	Other auxotrophies mutants
24	6	0.0005	0	−1.0000	Nuclear mutants
30	6	0.0014	1	−0.4992	Ubiquitin mediated proteolysis
22	5	0.0039	3	0.0129	Arginine and proline metabolism
83	10	0.0065	3	0.2921	Other cell wall mutants
19	4	0.0129	1	0.3544	Calcofluor white resistance
30	5	0.0131	5	−0.0005	Selenoamino acid metabolism
35	5	0.0131	0	−1.0000	Spindle mutants
35	5	0.0151	0	−1.0000	Other budding mutants
66	7	0.0183	12	0.0000	Starci and sucrose metabolism
72	8	0.0203	1	0.8109	Secretory mutants
14	3	0.0295	1	−0.2755	Methionine auxotrophy (Met)
48	6	0.0333	1	0.6699	Bud localization
72	7	0.0480	0	−1.0000	Actin cytoskeleton mutants
30	4	0.0595	2	−0.1480	Sulfur metabolism
115	9	0.0697	4	0.2653	Calcofluor white sensitivity
9	2	0.0705	0	−1.0000	Golgi mutants
34	4	0.0723	3	0.0412	G1 arrest
138	9	0.1528	8	−0.0130	Sporulation efficiency
80	6	0.1836	5	0.0349	Other cell morphology mutants
66	3	0.6253	4	0.0625	Osmotic sensitivity (Osm)
38	1	0.7617	5	−0.0016	Galactose metabolism
70	2	0.8295	5	−0.0210	MAPK signaling pathway
153	3	−0.9826	5	−0.0001	Divalent cations and heavy metals sensit.
48	1	−0.9006	4	0.0230	Silencing mutants
10	1	−0.4002	2	−0.0205	Cysteine metabolism
20	2	−0.2250	3	0.0099	Fatty acid metabolism
4	1	−0.1848	2	0.0030	Glutamate auxotrophy
1	1	−0.0498	0	−1.0000	Cell wall mutants
18	3	−0.0495	2	−0.0619	Nitrogen metabolism
17	5	−0.0011	4	−0.0005	Methionine metabolism
35	7	−0.0010	2	0.1886	Citrate cycle TCA_cycle
17	5	−0.0008	1	−0.3239	One carbon pool by folate
50	9	−0.0005	5	−0.0053	Glycine serine and threonine metab.

List of pathways that are most affected in at least one of the two microarray experiments This Pathway Processor Programm employs the Fisher Exact Test to measure the probability that a pathway is significantly altered, for a threshold of 1.8. The factors taken into account are: the number of ORFs whose expression is altered in each pathway, the total number of ORFs contained in the pathway, and the proportion of the ORFs in the genome contained in a given pathway. The color of the cube indicates the extent of the variation, based on the magnitude of the *P*-values and the sign, with red being up-regulated, green down-regulated, and yellow no change.

[a] This column lists the number of genes in the particular pathway present in the data file.

[b] This column lists the number of genes that passed the cutoff in the particular pathway. In parenthesis is listed the fold change range that was entered when the program was run.

[c] F:ET. Fisher Exact Test (−1.8, 1.8).

analysis indicates that 8 out of the 21 pathways with p values less than 0.05 in T1 are involved in cell wall structure, actin cytoskeleton and spindle body ("cell-wall mutants", "Other cell-wall mutants", "calcofluor white resistance", secretory mutants" "spindle mutants", "other budding mutants", "bud localization" and "actin cytoskeleton mutants"). This effect exists in part, although attenuated, also in T2 ("other cell morphology mutants").

As reported by Gasch et al. [14], yeast cells respond to environmental changes by altering the expression of thousands of genes, displaying a genomic expression program. The Gasch program includes features that are specific to each stress, and features that respond in a stereotypical manner following environmental stress, referred to as Environmental Stress Response (ESR). When we clustered the 100 genes in common at the 1.5fold threshold between T1 and T2 with the Gasch results (Fig. 5) it became evident that at the transcriptional level the expression response elicited by Esc 1–21 resembled the response to osmotic shock induced with sorbitol. In particular, we found *GSY2* (glycogen synthase, YLR258W) and the phosphoglucomutase *PGM2*(YMR105C) up-regulated after 90 min of treatment, as reported after sorbitol osmotic stress, and *ENA2*(YDR039C), a gene important for salt tolerance. We found the *GPD1*(YDL022W), a glycerol 3P dehydrogenase involved in the HOG response up-regulated both in T1 and T2. This fact could justify down-regulation of the enzymes of the lower part of glycolysis found in the 2D gel experiments and in the transcriptional analysis (Supplementary Table 3), suggesting the production of glycerol as an osmoprotectant. The fact that Esc1–21 long-term response and adaptation mechanisms involved regulation of cell membrane structure and permeability is also indicated by the observation that 48 of the 88 genes showing the same trend in T1 and T2 are localized to the cellular, endoplasmic, mitochondrial, or nuclear membranes, and 10 are important for membrane folding or stability. We found up-regulated genes involved in trehalose synthesis (*TPS1*(YBR126C), *TPS2* (YDR074W) and *TSL1*(YML100W)) (Table 4) associated with osmotic shock. The induction of genes important for resistance to osmotic stress could prompt the cell to respond to osmotic stress and explain the tolerance of treated cells to exposure to 0.6 M sorbitol (Fig. 2, panel A). Not only the trehalose genes but other genes involved in the cold and heat shock response and sensitivity (Table 4) were differentially expressed upon treatment with Esc1–21. A number of additional cold and heat shock proteins (*HSP42* (YDR171W), *HSP104* (YLL026W), *HSP12* (YFL014W), *SSE2*(YBR169C)), were also up-regulated in T2 with respect to T1. An opposite trend was shown by *KAR2* (YJL034W) and other HSPs of the Hsp70s group*2,* the expression of which is about 2fold down-regulated in T1 together with 18 other heat response genes, including *OLE1* (YGL055W), a gene required for resistance to heat, heavily repressed in T1 (−2.5fold) and T2 (−4fold). The class of the cell-wall proteins often expressed upon stress or stationary phase was significantly affected: *CWP1*(YKL096W), a member of the SPR (serine/alanine rich proteins) and important constituent of the cell-wall, was up-regulated. *PSA1*(YDL055C), a GDP-mannose pyrophosphorylase required for normal cell-wall structure, was repressed in T1 and activated in T2.

As shown in Table 4, genes involved in DNA replication, inheritance, and G1-S transition were also affected in T1 ("Nuclear mutants class", "G1 arrest"), but not in T2. Nine of the 12 anti-correlated genes between T1 and T2 at the 1.5threshold (Supplementary Table 3) were important for cell division; one *CLN2*(YPL256C), a cyclin that affects G1/S transition of mitotic cell cycle, was repressed almost 3fold at T1 and slightly overexpressed at T2 (Table 5). The majority of genes affected by 45 min of Esc 1–21 treatment belonged to carbon metabolism (Supplementary Table 3). The up-regulated pathways were: "carbohydrate–lipid biosynthesis defects", "other carbon auxotrophies", "starch and sucrose metabolism"; the down-regulated were "one carbon pool by folate", "TCA cycle".

4. Discussion

In this study we report the biological effects of Esc 1–21 on *S. cerevisiae.* The results suggest that exposure of *S. cerevisiae* to sub-lethal levels of Esc 1–21 inflicts growth inhibition in the W303-1A strain. In particular, a 3h treatment with 50 μM Esc 1–21 induces reversible cell growth arrest: in fact after 6 h the effect disappears and cells start to grow again. Moreover, the treated cells show an abnormal morphology. Our profound knowledge of *S. cerevisiae* biology and genomics and the availability of atlases of gene transcription upon exposure to various stresses make *S. cerevisiae* an ideal candidate for investigation of the genomic and proteomic effects of Esc 1–21.

Comparative proteomic studies reveal that the yeast strain treated with Esc 1–21 for two different time, has a different protein expression pattern. Indeed we found both qualitative and quantitative differences between the treated and untreated cell line. In particular the 2D gel analysis identifies an early more dramatic proteomic response after 45 min and an adaptation to the drug after 90 min of treatment; the same trend is true for the transcriptional response.

The Esc 1–21 treatment induces expression of important genes involved in the osmotic shock response, prompting the cells to resist and adapt to osmotic stress; in fact *GPD1* (YDL022W) a glycerol 3P dehydrogenase, which is also involved in down-regulation of the enzymes of the lower part of glycolysis, is up-regulated. Moreover, the changes in TCA cycle highlighted by the expression analysis are in agreement with the results of the proteomic analysis: the absence of Adh1p, Eno2p, Pdc1p and Pyk1p proteins agrees with the down-regulation of the lower part of glycolysis associated with an overproduction of glycerol. The expression response elicited by Esc 1–21 resembles the response to osmotic shock induced with sorbitol. These data are in agreement with the cluster between the 100 genes involved in Esc 1–21 treatment and the Gasch results. Moreover, by analyzing the cell response to heat and osmotic stress, we reveal that treatment with the peptide at high concentration, induces an increase in osmotic tolerance and a decrease in heat stress resistance in comparison to the control. These results suggest, supported by

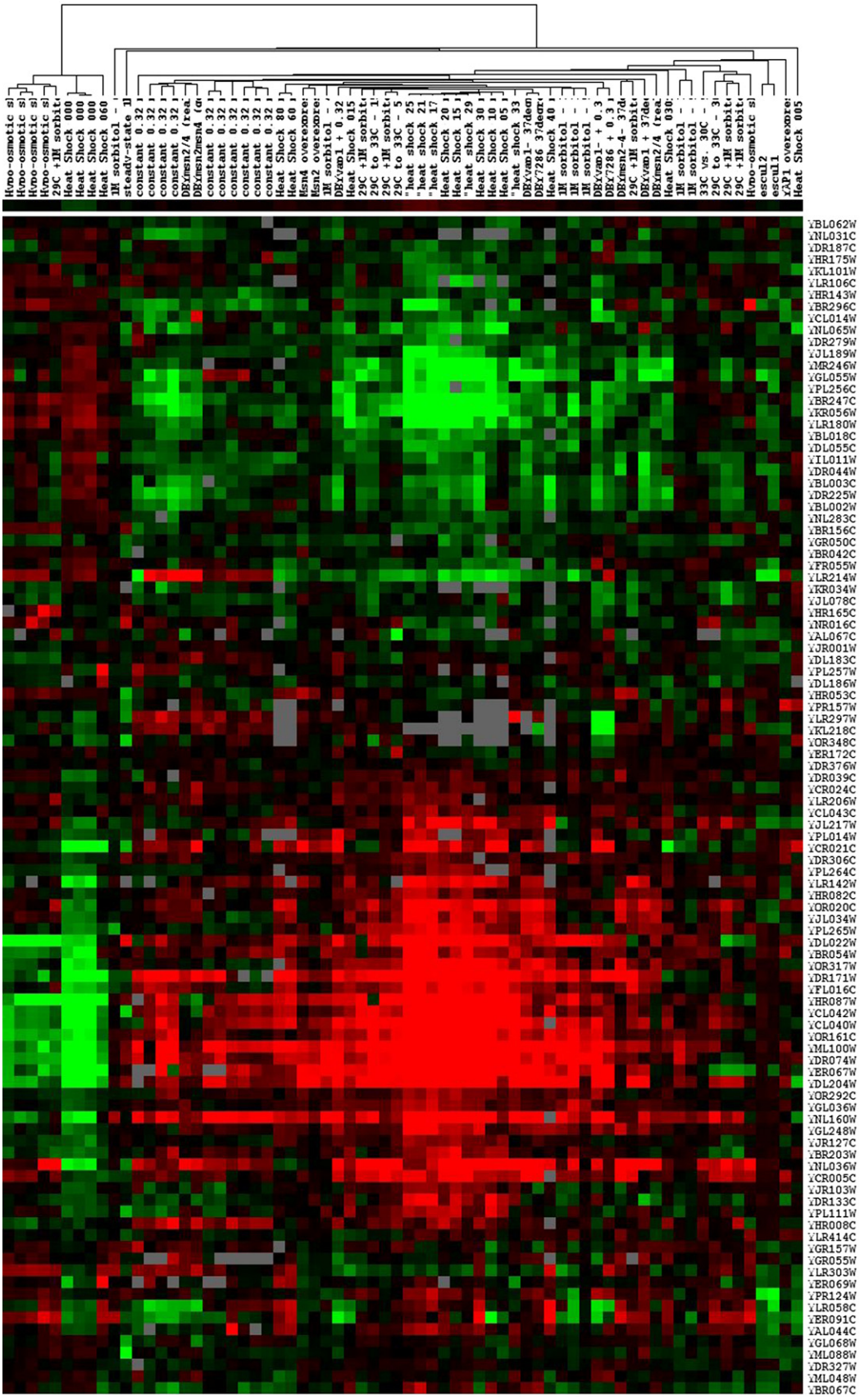

Fig. 5. Genomic expression program in response to Esc 1–21 treatment. Hierarchial cluster of the hundred genes in common at the 1.5fold threshold between T1 and T2 with Gasch results (14). The average expression of genes induced in each response is depicted by a red curve, while the average expression of genes repressed in each response is depicted by a green curve.

Table 4
Heat shock proteins and cell wall architecture

ORF	Gene name	T1	T2	Description
YGL055W	OLE1	−2.514950249	−3.967436273	Heat-sensitivity (ts)
YKL154W	SRP102	−2.168839596	−1.134011221	Heat-sensitivity (ts)
YJL034W	KAR2	−2.020689748	−1.582830694	Hsps
YNL312W	RFA2	−2.006329219	−1.013886737	Heat-sensitivity (ts)
YML130C	ERO1	−1.983057586	−1.366006365	Heat-sensitivity (ts)
YJR045C	SSC1	−1.956032598	−1.324720330	Heat- sensitivity (ts)
YLL024C	SSA2	−1.827919026	−1.424091411	Hsps
YDL090C	RAM1	−1.824372456	−1.148413362	Heat-sensitivity (ts)
YAL005C	SSA1	−1.785754408	−1.265772595	Hsps
YGL092W	NUP145	−1.769861054	−1.118227262	Heat-sensitivity (ts)
YGR075C	PRP38	−1.724137299	−1.128163139	Heat-sensitivity (ts)
YPR057W	BRR1	−1.666970661	1,052314234	Cold-sensitivity (cs)
YLR259C	HSP60	−1.441583957	−1.627503783	Hsps
YNL030W	HHF2	−1.381353680	1.830548991	Heat-sensitivity (ts)
YGR249W	MGA1	−1.366193106	1.509880327	Hsps
YIL119C	RPI1	1.099145481	1.848482669	Heat-sensitivity (ts)
YFL014W	HSP12	1.158258683	1.598167070	Hsps
YGR088W	CTT1	1.169137356	1.611324318	Hsps
YLL026W	HSP104	1.180969638	1.757001022	Heat-sensitivity (ts)
YMR105C	PGM2	1.216699699	2.001660866	Hsps
YBR169C	SSE2	1.363372751	1.693917403	Heat-sensitivity (ts)
YPL268W	PLC1	1.444267099	1.542719774	Heat-sensitivity (ts)
YBR126C	TPS1	1.466983218	2.087014767	Hsps
YOR181W	LAS17	1.504081633	1.306646608	Heat-sensitivity (ts)
YOR211C	MGM1	1.549712954	1.091734562	Heat-sensitivity (ts)
YFL016C	MDJ1	1.564645812	1.691647446	Heat-sensitivity (ts)
YLR430W	SEN1	1.573012391	1.243387452	Heat-sensitivity (ts)
YGR162W	TIF4631	1.601982812	1.021727456	Heat-sensitivity (ts)
YDR074W	TPS2	1.611949317	1.932226779	Heat-sensitivity (ts)
YOL081W	IRA2	1.620494637	−1.092208172	Heat shock sensitività
YGL073W	HSF1	1.626789452	1.255198045	Heat-sensitivity (ts)
YML100W	TSL1	1.645946551	3.046649408	Hsps
YAL009W	SPO7	1.646868648	−1.258713073	Heat-sensitivity (ts)
YFR036W	CDC26	1.664529817	−1.338304677	Heat-sensitivity (ts)
YDR171W	HSP42	1.666049998	2.214307116	Hsps
YLR148W	PEP3	1.673565607	−1.085083382	Heat-sensitivity (ts)
YOR036W	PEP12	1.829382852	1.445244992	Heat-sensitivity (ts)
YKL139W	CTK1	1.878224081	−1.322494375	Cold-sensitivity (cs)
YHR008C	SOD2	1.886487506	1.501246435	Hsps
YPL076W	GPI2	1.919545888	1.132747781	Heat-sensitivity (ts)
YDR212W	TCP1	2.177241214	−1.267188259	Cold-sensitivity (cs)
YDL108W	KIN28	2.243758391	1.277810306	Heat-sensitivity (ts)
YCR021C	HSP30	2.369063970	2.957385261	Hsps
YBR054W	YRO2	2.763741176	4.321713172	Hsps
YOR181W	LAS17	1.504081633	1.306646608	Actin cytoskeleton mutants
YDR129C	SAC6	1.571958469	1.113226862	Actin cytoskeleton mutants
YPL242C	IQG1	1.676489888	−1.012082363	Actin cytoskeleton mutants
YIL034C	CAP2	1.859005186	−1.009900152	Actin cytoskeleton mutants
YLR319C	BUD6	1.743198687	1.134833987	Actin cytoskeleton mutants
YKL092C	BUD2	1.595132092	−1.104366102	Bud localization
YCL014W	BUD3	1.662970392	1.620792915	Bud localization
YHR023W	MYO1	2.18327365	1.037450824	Bud localization
YPR159W	KRE6	1.612626036	1.446226651	Calcofluor white sensitività
YBL039C	URA7	1.752831474	−1.130567535	Calcofluor white sensitività
YKL096W	CWP1	2.350995193	1.243452521	Calcofluor white sensitività
YPL053C	KTR6	2.888244302	−1.232483650	Calcofluor white sensitività
YDL055C	PSA1	−1.726988324	1.593427773	Calcofluor white sensitività

*T1 and T2 are the ratio values of expression measured using DNA microarrays, after 45 (T1) and 90 min (T2) of treatment with 50 μM Esc 1–21, relative to the untreated control.

List of genes under/overexpressed commonly in treated for 45 (T1) or 90 (T2) min or untreated W303-1A yeast cells. These genes belong to the heat shock protein class or are involved in the cell wall synthesis. The average expression of genes induced in each response is depicted by a red curve, while the average expression of genes repressed in each response is depicted by a green curve.

Table 5
Cell cycle progression

ORF	Gene name	T1	T2	Description
YHR143W	DSE2	−2.258846901	1.711273337	Cell separation after division
YOR264W	DSE3	−1.061002763	1.533342390	Cell separation after division
YNR067C	DSE4	1.146676096	1.684069769	Cell separation after division
YFL009W	CDC4	1.578331374	1.179471553	Cell_cycle
YMR199W	CLN1	−1.497565204	−1.063466642	Cell_cycle
YPL256C	CLN2	−2.683740389	1.534800914	Cell_cycle
YAL040C	CLN3	1.550936627	1.091946413	Cell_cycle
YEL032W	MCM3	1.913170813	−1.491253783	Cell_cycle
YBR136W	MEC1	1.751014597	−1.278571801	Cell_cycle
YDL106C	PHO2	2.067880981	1.022235688	Cell_cycle
YGL073W	HSF1	1.626789452	1.255198045	G1 arrest
YDL090C	RAM1	−1.824372456	−1.148413362	G1 arrest
YBR079C	RPG1	1.203181800	1.598582341	G1 arrest
YGR113W	DAM1	1.573608771	−1.186341119	Nuclear mutants
YOR341W	RPA190	1.961643272	1.468610241	Nuclear mutants
YGL097W	SRM1	1.569630394	−1.054987682	Nuclear mutants
YNL172W	APC1	1.661699833	1.003822668	Other cell cycle defects
YPL255W	BBP1	1.680877826	1.184753426	Other cell cycle defects
YGL116W	CDC20	1.090918062	−1.710055976	Other cell cycle defects
YJL090C	DPB11	1.854560705	1.440901265	Other cell cycle defects
YDR225W	HTA1	−2.110501443	1.632088164	Other cell cycle defects
YBL003C	HTA2	−2.025356889	1.541746497	Other cell cycle defects
YDR224C	HTB1	−1.247974758	1.719786184	Other cell cycle defects
YBL002W	HTB2	−1.797374624	1.622885897	Other cell cycle defects
YPL242C	IQG1	1.676489888	−1.012082363	Other cell cycle defects
YHR023W	MYO1	2.018327365	1.037450824	Other cell cycle defects
YLR234W	TOP3	2.084865629	1.119931847	Other cell cycle defects
YMR232W	FUS2	1.509355846	−1.018141309	Mating
YBL016W	FUS3	−1.506473213	−1.371792359	Mating
YMR096W	SNZ1	−2.494679903	−1.358682944	Mating efficiency
YOL051W	GAL11	−2.822002081	−1.075322109	Other mating and sporulation defects
YPL082C	MOT1	1.729792886	1.338219385	Other mating and sporulation defects
YLR195C	NMT1	−1.751439086	−1.409149698	Other mating and sporulation defects
YJL090C	DPB11	1.854560705	1.440901265	DNA metabolism
YEL032W	MCM3	1.913170813	−1.491253783	DNA metabolism
YOR341W	RPA190	1.961643272	1.68610241	DNA metabolism
YPR102C	RPL11A	−1.740430102	−1.004136653	Ribosome
YNL301C	RPL18B	1.510572929	1.045580817	Ribosome
YPL220W	RPL1A	−1.677968039	−1.145753095	Ribosome
YOR234C	RPL33B	−1.986187881	1.097601390	Ribosome
YJL189W	RPL39	1.516860779	1.617257491	Ribosome
YJL191W	RPS14B	1.543522357	1.021903384	Ribosome
YLR441C	RPS1A	−2.060019943	−1.009593271	Ribosome
YKL156W	RPS27A	−1.879637034	1.005984458	Ribosome
YGR184C	UBR1	1.840213032	1.084619388	Ubiquitin mediated proteolysis
YJL197W	UBP12	2.091196193	1.020828913	Ubiquitin mediated proteolysis
YIL156W	UBP7	1.787027682	−1.017903964	Ubiquitin mediated proteolysis
YKL145W	RPT1	1.164930681	−1.538789092	Ubiquitin mediated proteolysis

*T1 and T2 are the ratio values of expression measured using DNA microarrays, after 45 (T1) and 90 min (T2) of treatment with 50 μM Esc 1–21, relative to the untreated control.

List of genes under- or overexpressed at both time points. These genes are involved in the cell cycle related processes. The average expression of genes induced in each response is depicted by a red curve, while the average expression of genes repressed in each response is depicted by a green curve.

the gene expression analysis, that Esc 1–21 acts on yeast cell-wall integrity, triggering some of the responses of hyper-osmotic shock through the HOG pathway. In agreement with this, specific members of the heat shock protein class are also affected. This may account for the increased sensitivity of W303-1A cells to heat shock. An alternative hypothesis for the increased sensitivity of pre-treated cells to heat shock could be that the activation of the HOG pathway results in increased production of glycerol and thus increased turgor. Increasing the temperature increases the fluidity of the plasma membrane. Together, they result in a further decrease in plasma membrane integrity.

The transient change in expression of treated cells at 45 min affects a number of genes encoding proteins that respond to physiological processes associated with DNA metabolism, chromosome structure and histone metabolism. This picture is

consistent with the reversible cell growth arrest caused by drug-induced defects of cell wall and cell membranes.

Repression of actin synthesis in treated cells is one of the major results of proteomic analyses and has been confirmed by Western blot. This result is in agreement with the report from Ja Choon Koo [9], showing that Pn-AMP1, an antimicrobial peptide from *Pharbitis nil*, induces rapid depolarization of actin cables in *S. cerevisiae* and *Candida albicans*. The absence of actin in the 2D gels could be the cause of the compensatory overexpression at 45 min of genes involved in the actomyosin ring, actin cytoskeleton and spindle body formation, actin patch assembly, as well as seven other genes responsible for the progression of bud separation. In our experiments, only in three cases out of 5 were gene expression data correlated with proteomic results. Nevertheless it has to be considered that we are not in steady-state conditions and that changes in the expression level cannot allow us to appreciate the effects of protein turnover and degradation. For example, although Act1 protein is absent after Esc 1–21 treatment, the expression of the *ACT1* (YFL039C) gene is not changed. This could be the result of compensatory effects associated with a direct insult to the protein actin (degradation, modification). We can conclude that Esc 1–21 induces membrane perturbation through specific interaction with negatively charged phospholipids. Previous reports indicate that a conserved group of cationic antimicrobial peptides, plant defensine, exert their antifungal effect by inducing membrane permeabilization [27]. We conclude that only a comparative analysis associating gene expression with proteomic results can provide complete understanding of the effects of a drug.

Acknowledgments

This work was supported by a MIUR-PRIN 2003 and MIUR-PRIN 2005 (to A. Modesti and M. Simmaco) grants and partially by the Cassa di Risparmio di Firenze (to A. Modesti). This work was also supported by Duccio Cavalieri from DC-Thera Contract no. 512074 LSHB-CT-2004-512074 and by Tania Gamberi from the Network of Excellence in Nutrigenomics. We thank Donatella Barra and Piero Dolara for critical reading of the manuscript.

Appendix A. Supplementary data

Supplementary data associated with this article can be found, in the online version, atdoi:10.1016/j.bbapap.2007.04.006.

References

[1] H.G. Boman, Antibacterial peptides: basic facts and emerging concepts, J. Intern. Med. 254 (2003) 197–215.
[2] H.G. Boman, Peptide antibiotics and their role in innate immunity, Annu. Rev. Immunol. 13 (1995) 61–92.
[3] T. Ganz, Defensins: antimicrobial peptides of innate immunity, Nat. Rev., Immunol. 3 (2003) 710–720.
[4] M. Zasloff, Antimicrobial peptides of multicellular organisms, Nature 415 (2002) 389–395.
[5] R.E.W. Hancock, A. Patrzykat, Clinical development of cationic antimicrobial peptides:from natural to novel antibiotics, Curr. Drug. Targets Infect. Disord. 2 (2002) 79–83.
[6] J. Harder, J.M. Schroder, Antimicrobial peptides in human skin, Chem. Immunol. Allergy 86 (2005) 22–41.
[7] R.E. Hancock, A. Rozek, Role of membranes in the activities of antimicrobial cationic peptides, FEMS Microbiol. Lett. 206 (2002) 143–149.
[8] Y. Shai, Mode of action of membrane active antimicrobial peptides, Biopolymers 66 (2002) 236–248.
[9] J.C. Koo, B. Lee, M.E. Young, S.C. Koo, J.A. Cooper, D. Baek, C.O. Lim, S.Y. Lee, D.J. Yun, M.J. Cho, Pn-AMP1, a plant defense protein, induces actin depolarization in yeasts, Plant Cell Physiol. 45 (2004) 1669–1680.
[10] M. Simmaco, G. Mignogna, D. Barra, Antimicrobial peptides from amphibian skin: what do they tell us? Biopolymers 47 (1998) 435–450.
[11] M.L. Mangoni, R. Miele, T.G. Renda, D. Barra, M. Simmaco, The synthesis of antimicrobial peptides in the skin of *Rana esculenta* is stimulated by microorganisms, FASEB J. 15 (2001) 1431–1432.
[12] M. Simmaco, G. Mignogna, D. Barra, F. Bossa, Antimicrobial peptides from skin secretions of *Rana esculenta*, molecular cloning of cDNAs encoding esculentin and brevinins and isolation of new active peptides, J. Biol. Chem. 269 (1994) 11956–11961.
[13] M.L. Mangoni, D. Fiocco, G. Mignogna, D. Barra, M. Simmaco, Functional characterisation of the 1–18 fragment of esculentin-1b, an antimicrobial peptide from *Rana esculenta*, Peptides 24 (2003) 1771–1777.
[14] A.P. Gasch, P.T. Spellman, C.M. Kao, O. Carmel-Harel, M.B. Eisen, G. Storz, D. Botstein, P.O. Brown, Genomic expression programs in the response of yeast cells to environmental changes, Mol. Biol. Cell 11 (2000) 4241–4257.
[15] S.E. Schaus, D. Cavalieri, A.G. Myers, Gene transcription analysis of *Saccharomyces cerevisiae* exposed to neocarzinostatin protein–chromophore complex reveals evidence of DNA damage, a potential mechanism of resistance, and consequences of prolonged exposure, Proc. Natl. Acad. Sci. U. S. A. 98 (2001) 11075–11080.
[16] A. Kolkman, M.M.A. Olsthoorn, C.E.M. Heeremans, A.J.R. Heck, M. Slijper, Comparative proteome analysis of *Saccharomyces cerevisiae* grown in chemostat cultures limited for glucose or ethanol, Mol. Cell. Proteomics 4 (2005) 1–11.
[17] A. Modesti, L. Bini, L. Carraresi, F. Magherini, S. Liberatori, V. Pallini, G. Manao, L.A. Pinna, G. Raugei, G. Ramponi, Expression of the small tyrosine phosphatase (Stp1) in *Saccharomyces cerevisiae*: a study on protein tyrosine phosphorylation, Electrophoresis 22 (2001) 576–585.
[18] C.M. Grozinger, E.D. Chao, H.E. Blackwell, D. Moazed, S.L. Schreiber, Identification of a class of small molecule inhibitors of the sirtuin family of NAD-dependent deacetylases by phenotypic screening, J. Biol. Chem. 276 (2001) 38837–38843.
[19] D.F. Hochstrasser, A. Patchornick, C.R. Merril, Development of polyacrylamide gels that improve the separation of proteins and their detection by silver staining, Anal. Biochem. 173 (1998) 412–423.
[20] A. Shevchenko, M. Wilm, O. Vorm, M. Mann, Mass spectrometric sequencing of proteins from silver-stained polyacrylamide gels, Anal. Chem. 68 (1996) 850–858.
[21] P. Grosu, J.P. Townsend, D.L. Hartl, D. Cavalieri, Pathway Processor: a tool for integrating whole-genome expression results into metabolic networks, Genome Res. 12 (2002) 1121–1126.
[22] D. Cavalieri, J.P. Townsend, D.L. Hartl, Manifold anomalies in gene expression in a vineyard isolate of *Saccharomyces cerevisiae* revealed by DNA microarray analysis, Proc. Natl. Acad. Sci. U. S. A. 97 (2000) 12369–12374.
[23] T. Komiyama, T. Otha, H. Urakami, Y. Shiratori, T. Takasuka, M. Satoh, T. Watanabe, Y. Furuichi, Pore formation on proliferating yeast *Saccharomyces cerevisiae* cell buds by HM-1 killer toxin, J. Biochem. (Tokyo) 119 (1996) 731–736.
[24] K. Irie, M. Takase, K.S. Lee, D.E. Lavin, H. Araki, K. Matsumoto, Y. Oshima, MKK1 and MKK2, which encode *Saccharomyces cerevisiae* mitogen-activated protein kinase–kinase homologs, function in the pathway mediated by protein kinase C, Mol. Cell. Biol. 13 (1993) 3076–3083.
[25] L.J. Garcia-Rodriguez, A. Duran, C. Roncero, Calcofluor antifungal action depends on chitin and a functional high-osmolarity glycerol response

(HOG) pathway: evidence for a physiological role of the *Saccharomyces cerevisiae* HOG pathway under noninducing conditions, J. Bacteriol. 182 (2000) 2428–2437.

[26] Y. Kamada, U.S. Jung, J. Piotrowski, D.E. Levin, The protein kinase C-activated MAP kinase pathway of *Saccharomyces cerevisiae* mediates a novel aspect of the heat shock response, Genes Dev. 9 (1995) 1559–1571.

[27] W.H. Mager, M. Siderius, Novel insight into the osmotic stress response of yeast, FEMS Yeast Res. 2 (2002) 251–257.

[28] A. Zakrzewska, A. Boorsma, S. Brul, K.J. Hellingwerf, F.M. Klis, Transcriptional response of *Saccharomyces cerevisiae* to the plasma membrane-perturbing compound chitosan, Eukaryot. Cell 4 (2005) 703–715.